POLITECNICO DI TORINO
Repository ISTITUZIONALE

TCAD Simulations of Degradation Mechanism in p-GaN Gate HEMTs under Gate Stress

Original
TCAD Simulations of Degradation Mechanism in p-GaN Gate HEMTs under Gate Stress / De Ruvo, E., Guerrieri, S.D., Bonani, F., Cornigli, D., Larcher, L.. - ELETTRONICO. - (2026), pp. 1-6. (2026 IEEE International Reliability Physics Symposium (IRPS) Tucson (USA) 22-26 March 2026) [10.1109/irps61424.2026.11499242].

Availability:
This version is available at: 11583/3012008 since: 2026-06-14T04:16:09Z

Publisher:
IEEE

Published
DOI:10.1109/irps61424.2026.11499242

Terms of use:

This article is made available under terms and conditions as specified in the corresponding bibliographic description in the repository

Publisher copyright
IEEE postprint/Author's Accepted Manuscript

©2026 IEEE. Personal use of this material is permitted. Permission from IEEE must be obtained for all other uses, in any current or future media, including reprinting/republishing this material for advertising or promotional purposes, creating new collecting works, for resale or lists, or reuse of any copyrighted component of this work in other works.

(Article begins on next page)

19 June 2026

TCAD Simulations of Degradation Mechanism in p-GaN Gate HEMTs under Gate Stress

Edoardo De Ruvo*, Simona Donati Guerrieri, Fabrizio Bonani
Department of Electronics and Telecommunications
Politecnico di Torino
Torino, Italy
*e-mail: edoardo.deruvo@polito.it

Davide Cornigli, Luca Larcher
Applied Materials Inc.
CA, USA

***Abstract*— In this paper we perform physical simulations to study the time-dependent-gate-breakdown (TDGB) phenomenon of *p*-GaN gate HEMTs subject to constant-voltage stress (CVS). Leveraging on the advanced capabilities of Ginestra TCAD software, we show for the first time a simulation methodology that is able to model and explain the onset of gate breakdown that is experimentally measured in these devices during a CVS. In our simulations we activate the thermochemical model for the defect generation which, due to a strongly field-dependent rate, creates traps in the *p*-GaN close to the gate contact resulting in the gate current increase. We also perform a statistical analysis of this phenomenon and we show how, by adding randomization effects in the simulation, we can also reproduce the temporal dispersion of breakdown events.**

***Index Terms*— Breakdown, p-GaN HEMTs, Reliability, TCAD, Traps.**

I. Introduction

Normally-off GaN HEMTs exploiting a *p*-GaN gate are promising devices in power electronics: with respect to other enhancement-mode architectures, they can be fabricated with a low-cost process and allow for a lower gate leakage current. The gate contact can be either ohmic or Schottky, the latter one being preferred to further reduce the leakage current, because the metal/*p*-GaN Schottky diode is reversely biased in normal operating conditions [1]-[3]. However, these devices possess a low gate-breakdown voltage, which limits the maximum applicable gate voltage swing, ultimately imposing significant constraints on the gate driver design [4], [5].

There is still a debate about the precise physical mechanism which initiates the breakdown. In [4], [6] it is traced back to the avalanche breakdown initiated by impact ionization in the *p*-GaN depleted region, where a very strong electric field is present due to the high Mg doping. Many works instead agree that breakdown is tightly connected to defect generation, still caused by the high electric field in the *p*-GaN region, then leading to a sudden increase of gate current, possibly through a percolation path [4], [7], [8]. The role of defects is also supported by the fact that a link has been observed between the breakdown and the gate current at the beginning of stress, which is in turn closely related to material defectiveness [4], [9].

Another important point to note for understanding the breakdown phenomenon is the time-to-breakdown (t_{BD}) behavior vs. temperature: conflicting experimental results are present in the literature. On one side, some [10]-[13] observed that t_{BD} increases with temperature, while others [4], [8], [14] measured a negative behavior. Reference [9] even demonstrates that different fabrication procedures lead to opposite results in terms of temperature behavior. It is therefore evident that different physical effects are at play in these devices, and their relative importance, which determines the final behavior of the device, is deeply influenced by the specific technology employed.

It is therefore of fundamental importance to carry out physical (TCAD) simulations, which can shed light on the experimental measurement findings and therefore verify the physical mechanism that leads to breakdown. In this work we perform physical simulations of a *p*-GaN gate HEMT by exploiting Ginestra TCAD software [15]. We propose a novel

Figure 1. Reference structure [16], [17]. Red line: simulated section, i.e. a *p*-GaN/AlGaN/GaN heterostructure. A 5 nm × 5 nm cross section is considered for 3D simulations.

modeling technique to simulate the device degradation under forward-bias constant gate stress, by using the thermochemical model for the defect generation in the *p*-GaN layer. Simulation results show that the model is able to explain the TDGB, i.e. the sudden increase of gate current measured experimentally under CVS. Moreover, by including an additional randomization effects in the dopant distribution, we obtain a Weibull distribution whose β parameter agrees with the experimental one.

II. Simulation Framework

In this analysis we consider a typical *p*-gate structure, focusing in particular on the device demonstrated in [16], [17], and we study a 1D vertical section of the gate stack, i.e. a GaN/AlGaN/*p*-GaN heterostructure, see Fig. 1; device parameters are summarized in Table 1.

Device parameters used in simulations

Parameter	Description	Value
ϕ_{M}	Metal workfunction of the gate Schottky contact	5.2 eV
N_{D}	Background *n*-doping	10^{15} cm^{-3}
N_{A}	Mg *p*-doping	3×10^{19} cm^{-3}
E_{Mg}	Energy level of Mg doping (partial ionization)	$E_{\mathrm{V}} + 0.2$ eV
σ_{pol}/q	Net polarization charge	9×10^{12} cm^{-2}

TABLE I.

To simulate the device, the commercially available software Ginestra from Applied Materials was used: this software is especially suited for the research purpose, being a multiscale, defect-centric simulation platform. Transient simulations were performed over a 3D mesh, considering a 5 nm × 5 nm cross section of the GaN/AlGaN/*p*-GaN heterostructure. The choice of this very small area allows for a 3D analysis including trap random generation; the simulation outcome is then scaled to the actual gate area when comparing to measured data. To study the onset of gate breakdown in *p*-GaN gate HEMTs, CVS tests were performed at different values of gate voltage. The gate current was simulated by including thermionic emission and direct tunneling in the simulations; concerning trap-assisted tunneling (TAT), it was considered as well among the possible charge transport mechanisms, but it was not activated because it was shown to yield a negligible contribution within our model, as will be explained in the following.

Degradation was simulated in the device under stress by activating the Ginestra thermochemical model for defect generation, according to which weak bonds are broken in the material at high electric field, thus creating defects [18]-[20]. Within this model, the field- and temperature-dependent bond-breakage rate (which then becomes the defect generation rate) is calculated as:

$$R_G(x,y,z) = \nu_0 \exp\left[-\frac{E_A - b\cdot F(x,y,z)}{k_B T}\right], \quad (1)$$

where ν_0 is the bond vibration frequency, E_A is the zero-field bond-breakage activation energy, $b = p_0 \cdot (2+\varepsilon_r)/3$ is the bond polarizability factor, p_0 is the polarizability, ε_r is the relative permittivity of the material, F is the electric field. Therefore, defects are randomly generated throughout the device following the generation rate, thanks to kinetic Monte-Carlo calculations. Being a stochastic process, CVS tests were repeated by using the Statistics panel in Ginestra, that allows to directly run multiple simulations and extract the results' statistics. In addition to the randomness of defect generation, extra randomization effects were added to study their impact on the time dispersion of breakdown events. This was possible since in Ginestra it is possible to randomize any parameter: in particular, randomization was activated on the energy level of traps created, on the initial number of traps and on the nominal level of Mg doping.

III. Simulation Results and Discussion

A preliminary calibration was carried out on the device by comparing gate leakage current simulations with the experimental data in [16]. The calibration was performed in the high-bias regime, since stress measurements are typically performed at high voltage. In this region, leakage is dominated by tunneling of holes at the Schottky contact [17], as represented in the band diagram in Fig. 2, while the effect of traps is minor: the high voltage calibration allowed us to extract the hole tunnelling mass, $0.3\,m_0$, while the electron

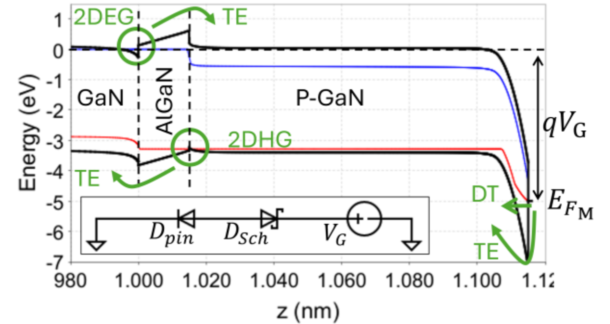

Figure 2. Energy-band diagram at $V_{\mathrm{G}} = 5$ V. Arrows show the possible leakage mechanisms: hole direct tunneling (DT) and thermionic emission (TE). Inset: equivalent circuit of the heterostructure consisting of two back-to-back diodes in series.

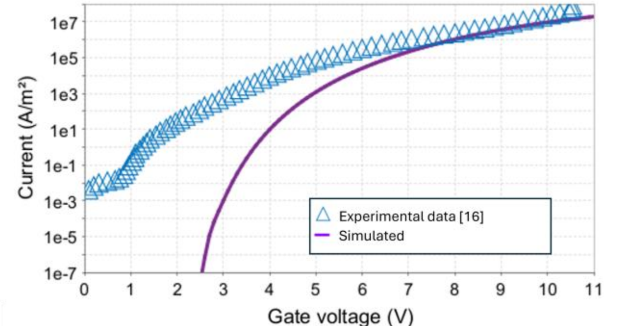

Figure 3. Simulated $I_{\mathrm{G}}(V_{\mathrm{G}})$ curve after calibration vs. experimental data [16].

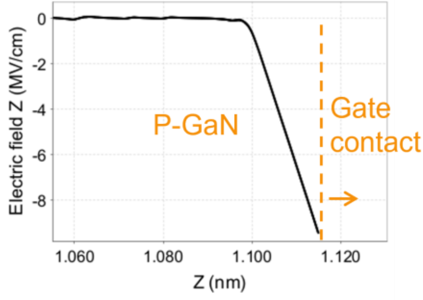

Figure 4. Electric field profile close to the p-GaN/Schottky contact interface at $V_G = 9$ V.

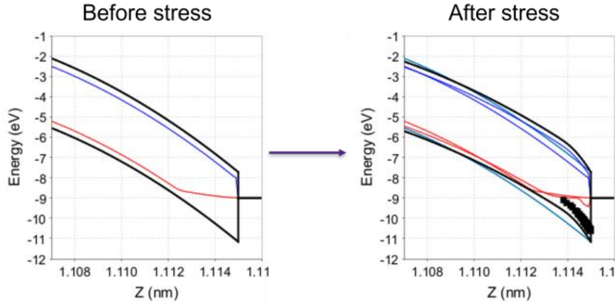

Figure 5. Energy-band diagram in p-GaN layer close to the gate contact (left) before and (right) after a constant voltage stress at $V_G = 9$ V. During the stress, traps are generated (black squares). Their effect is to bend the bands more with respect to the fresh device (black vs. light blue lines).

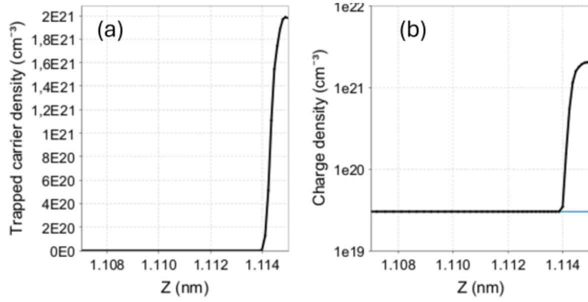

Figure 6. (a) Trapped carrier density in p-GaN close to the gate contact after a CVS at $V_G = 9$ V. (b) Charge density (light blue) before and (black) after the stress

tunneling mass is set to $0.1\ m_0$. The calibrated gate current is shown in Fig. 3.

A. Constant-voltage stress

As described in Section 2, degradation of materials during a CVS is simulated using the thermochemical model for defect generation according to the rate in (1). The model was activated only in the p-GaN layer, and the following parameters were chosen after tuning against experimental data of t_{BD} in [16]: $\nu_0 = 4.5 \cdot 10^{13}$ Hz , $E_A = 2.9$ eV , $p_0 = 5.25$ eÅ, and it is supposed that degradation leads to the creation of acceptor traps at $E_V + 0.2$ eV in p-GaN. Since the rate is field-dependent and the electric field is very strong only in the p-GaN/Schottky contact depleted region, as shown in Fig. 4, the trap generation mechanism is impactful only in a very thin p-GaN portion, very few nanometers below the interface.

Indeed, it can be seen in Fig. 5 that after the voltage stress, traps are generated very close to the contact, with a peak exactly at the interface. These traps, being acceptors below the

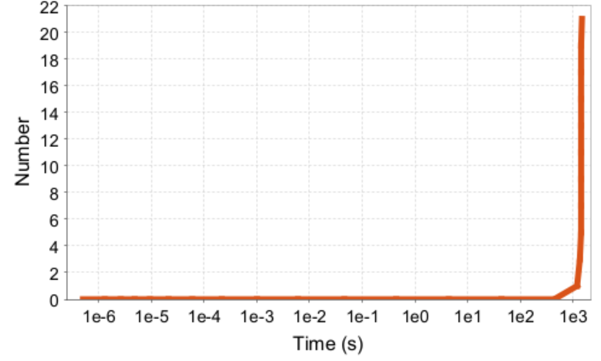

Figure 7. Transient of the total number of generated traps during a CVS at $V_G = 9$ V inside the 5 nm × 5 nm cross section of the heterostructure.

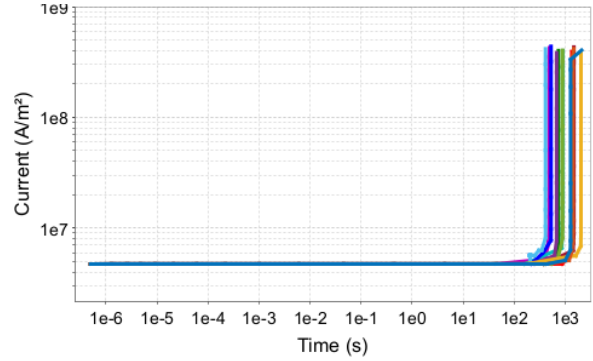

Figure 8. Statistical trials of stresses at $V_G = 9$ V.

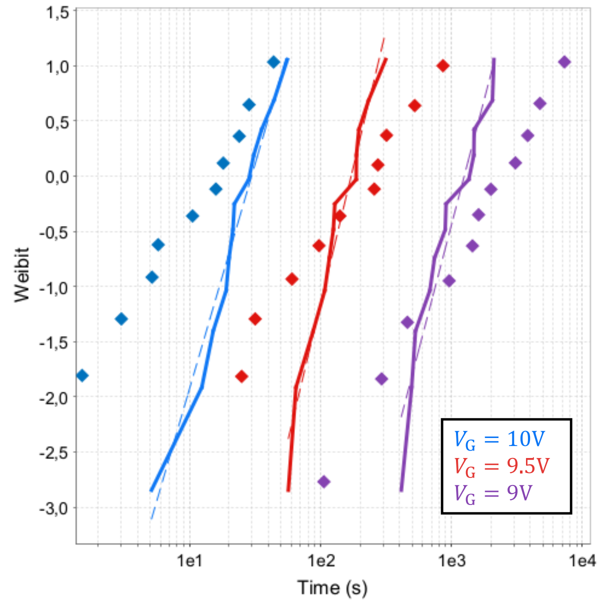

Figure 9. Weibull plot of t_{BD} at different voltages. Diamonds: experimental data [16], lines: simulation results, dashed lines: fitting of simulation results.

hole quasi-Fermi level, are completely ionized; therefore, the traps will contribute to the total charge with a fixed negative charge peaked at the interface, as shown in Fig. 6, left. This charge adds to the negative depletion charge due to the Mg doping, giving rise to a charge density increased by more than one order of magnitude in the last nanometer below the interface, see Fig. 6, right. Its effect is to further increase the electric field in the depleted region: finally, the most evident effect of this additional charge is to bend the bands even closer to the interface, and to make a thinner barrier (see again the band diagram in Fig. 5), drastically enhancing the tunneling of holes at the Schottky contact. This phenomenon is extremely rapid, as can be seen in the transient of the generated traps in Fig. 7, and makes sure that, as soon as the traps start to be generated, the gate current increases very rapidly, as shown in Fig. 8: remarkably, this phenomenon can explain the sudden increase in gate current that is observed in typical stress measurements [17].

Fig. 8 shows the repetition of the same simulation: here, the randomness of simulations clearly appear, due to the random trap generation, hence the need for a statistical analysis. For each trial, the time-to-breakdown was identified when current reaches the limit that had been set ($3 \times 10^8\,\mathrm{A/cm^2}$). After repeating the analysis for different voltages, the statistics of t_{BD} can be studied: Fig. 9 reports its Weibull plot. It can be seen that t_{BD} can be well described by a Weibull distribution, as verified experimentally [4], [5], [16]. However, with respect to measurements [16], the simulated Weibull curves are steeper, i.e. the β parameter is higher (more than three times larger than the experimental value 0.9 [16]): in other words, breakdown events happen too close together in time. Hence, an accurate modeling requires to ensure that breakdown events are more dispersed over time.

B. Addition of randomization effects

To obtain a larger temporal dispersion of breakdown events, and therefore reduce the β factor, some strategies have been attempted, all of which have in common the idea of adding further randomization effects that can enhance the randomness of breakdown phenomena:

- Randomization of the energy level of traps created during the stress.
- Randomization of the initial number of traps (initially, traps are not present in the fresh devices before the stress).
- Randomization of the nominal (chemical) level of Mg doping in *p*-GaN.

Our simulations show that the first strategy does not have a considerable effect. This is not surprising: since the generated traps have mainly an electrostatic effect, they do not conduct current by TAT, so traps at different levels are equivalent, as far as they are ionized. The physical conclusion is that there is a broad energy interval within the band gap of *p*-GaN, close to E_V, where traps can be generated and give rise to the same breakdown pattern.

The last two strategies, instead, are effective in increasing the time dispersion; qualitatively, they are very similar: indeed, they both have the effect of varying the sparce charge, and thus the band diagram, to finally act on the tunneling current of the fresh device.

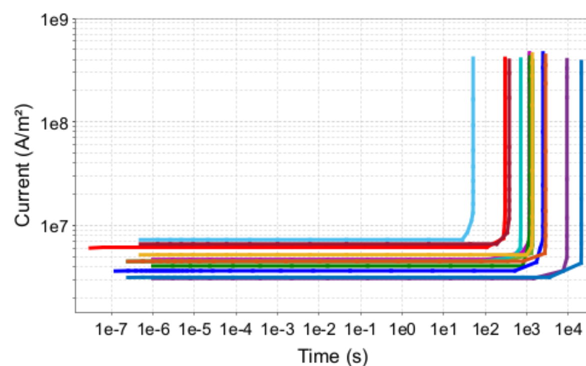

Figure 10. Statistical trials of stresses at $V_G = 9$ V with randomization of nominal level of Mg doping in *p*-GaN layer (gaussian distribution centered at the nominal value of $3 \times 10^{19}\ cm^{-3}$ and standard deviation of $10^{18}\ cm^{-3}$).

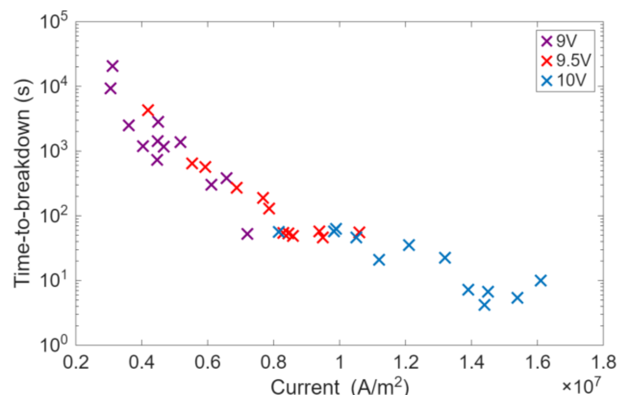

Figure 11. Dependence of time-to-breakdown on the initial gate current, extracted for different gate voltages

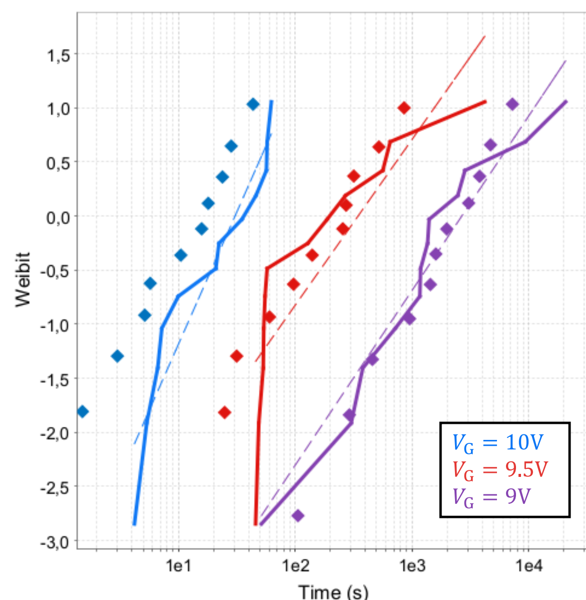

Figure 12. Weibull plot of t_{BD} at different voltages with randomization of doping level activated. Diamonds: experimental data [16], lines: simulation results, dashed lines: fitting of simulation results.

We discuss here as an example the results obtained following the third strategy, i.e. the randomization of the dopant concentration in p-GaN but, equivalently, also the activation of Mg dopants. The uncertainty of this parameter has been simulated by using a gaussian distribution peaked at the nominal value $3 \times 10^{19}\ \mathrm{cm}^{-3}$ with a standard deviation of $10^{18}\ \mathrm{cm}^{-3}$: in other words, devices of different trials have different (constant) values of Mg doping. Although this spread is moderate, simulations show that it can lead to an important effect; Fig. 10 shows the trials of current transients at fixed voltage: with respect to previous simulations (Fig. 8), it is evident how breakdown events are much more dispersed in time.

Due to the additional randomization effect, every device is different from the others: this can be noticed from the fact that different trials show different values of initial gate current, i.e. the current for the fresh device before stress. This consideration is important because it brings our simulations closer to reality where, since this technology is not fully mature, there is a noticeable difference between nominally identical devices: indeed, a significant spread in the initial value of the fresh device current is always observed [17]. In addition, it supports the observation that the initial gate current influences the breakdown time, again consistent with typical experimental data [4], [9]: Fig. 11 clearly shows that there is a decreasing trend for each set of simulations at a given voltage.

Fig. 12 shows the Weibull plot of t_{BD} after the addition of randomization effects: the enhanced time dispersion that was observed in Fig. 10 is of course reflected in a lower slope of Weibull curves and thus in a smaller β factor, that is now comparable to the experimental value [16].

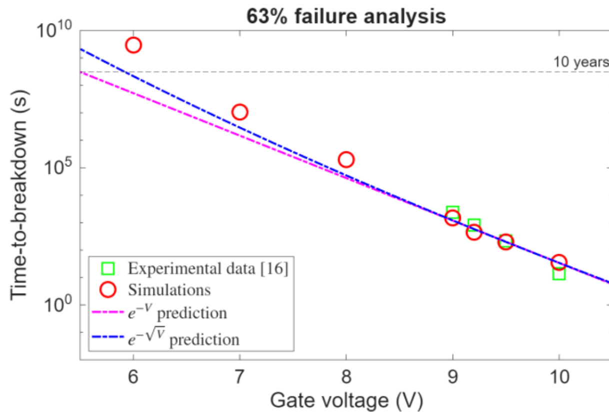

Figure 13. Lifetime prediction based on simulations and comparison with experimental data [16].

The last part of our work was aimed at obtaining the $t_{BD}(V_G)$ curve according to our model: Fig. 13 shows the simulated points, that were extended also to lower voltages. From a theoretical point of view, we expect a precise functional form for this curve: indeed, $t_{BD} \sim 1/R_G$, $R_G \sim e^F$, $F \sim \sqrt{V_G}$ (because it is a Schottky junction), so $t_{BD} \sim e^{-\sqrt{V_G}}$ and then $\log(t_{BD}) \sim -\sqrt{V_G}$: therefore, we expect the $\log(t_{BD}) - V_G$ relation not to be a perfect straight line. This is the reason why in Fig. 13 it can be observed that, by considering only the points at high voltage for the fitting, the $e^{-\sqrt{V_G}}$ prediction turns out to be a better fitting with respect to the e^{-V_G} one. In other words, it is confirmed that there is non-uniform slope of the function.

From this graph it is finally possible to extract the 10-years lifetime prediction at 63% failure, i.e. the maximum applicable voltage for a 10-years usage, which is a crucial parameter for the final use of the device: our model predicts 6.5 V.

IV. Conclusions

In this work we carried out physical simulations of CVS experiments on a cross section of the gate stack of a p-GaN gate HEMT. We proposed a novel modeling technique to simulate the TDGB of this device, adopting the thermochemical model for defect generation. During the stress, acceptor traps are created close to the valence band of p-GaN, in the immediate vicinity of the gate contact, where the field is maximum: their fixed charge causes the band bending to be more pronounced close to the interface, and consequently the hole tunneling is enhanced, finally resulting in a sudden increase of the gate current. By adding randomization effects in the device, we demonstrate that in our model it is also possible to tune the temporal spread of the breakdown events, i.e. the β parameter of the Weibull curves: in this way it is possible to obtain the same statistics measured experimentally.

This work paves the way for physical modeling and simulation of the TDGB, which may lead to a deeper understanding of this device. Future advances of this work could be the study of the temperature trend, the use of more advanced models that can couple the thermochemical description with the impact ionization, or the simulation of the entire transistor structure, in such a way to take into account perimeter/border effects.

Acknowledgment

This publication is part of the project PNRR-NGEU which has received funding from the MUR–DM630/2024.

References

[1] G. Greco, F. Iucolano, and F. Roccaforte, “Review of technology for normally-off HEMTs with p-GaN gate,” *Mater. Sci. Semicond. Process.*, vol. 78, pp. 96–106, May 2018, doi: 10.1016/j.mssp.2017.09.027.

[2] F. Roccaforte, G. Greco, P. Fiorenza, and F. Iucolano, “An overview of normally-off GaN-based high electron mobility transistors,” *Materials*, vol. 12, no. 10, p. 1599, May 2019, doi: 10.3390/ma12101599.

[3] Z. Wang et al., “Review on main gate characteristics of p-type GaN gate high-electron-mobility transistors,” *Micromachines*, vol. 15, no. 1, p. 80, 2024, doi: 10.3390/mi15010080.

[4] A. N. Tallarico et al., “Investigation of the p-GaN gate breakdown in forward-biased GaN-based power HEMTs,” *IEEE Electron Device Lett.*, vol. 38, no. 1, pp. 99–102, Jan. 2017, doi: 10.1109/LED.2016.2631640.

[5] I. Rossetto et al., “Field- and current-driven degradation of GaN-based power HEMTs with p-GaN gate: Dependence on Mg-doping level,” *Microelectronics Reliability*, vol. 76-77, pp. 298–303, 2017, doi: 10.1016/j.microrel.2017.06.061.

[6] T.-L. Wu et al., “Forward bias gate breakdown mechanism in enhancement-mode p-GaN gate AlGaN/GaN high-electron mobility transistors,” *IEEE Electron Device Lett.*, vol. 36, no. 10, pp. 1001–1003, Oct. 2015, doi: 10.1109/LED.2015.2465137.

[7] I. Rossetto et al., “Time-dependent failure of GaN-on-Si power HEMTs with p-GaN gate,” *IEEE Trans. Electron Devices*, vol. 63, no. 6, pp. 2334–2339, Jun. 2016, doi: 10.1109/TED.2016.2553721.

[8] M. Ťapajna, O. Hilt, E. Bahat-Treidel, and J. Würfl, “Gate reliability investigation in normally-off p-type-GaN cap/AlGaN/GaN HEMTs under forward bias stress,” *IEEE Electron Device Lett.*, vol. 37, no. 4, pp. 385–388, Apr. 2016, doi: 10.1109/LED.2016.2535133.

[9] M. Millesimo et al., “High-temperature time-dependent gate breakdown of p-GaN HEMTs,” *IEEE Trans. Electron Devices*, vol. 68, no. 11, pp. 5701–5706, Nov. 2021, doi: 10.1109/TED.2021.3111144.

[10] J. Yoon and H. Kim, “Investigation of temperature-dependent gate degradation in normally-off AlGaN/GaN high-electron-mobility transistor p-GaN,” Electronics, vol. 14, no. 9, p. 1764, 2025, doi: 10.3390/electronics14091764.

[11] X. Chao et al., “Investigation of the progressive gate breakdown behaviors in p-GaN gate HEMTs,” *IEEE Trans. Electron Devices*, vol. 70, no. 1, pp. 25–30, Jan. 2023, doi: 10.1109/TED.2022.3220498.

[12] M. Fregolent et al., “Negative Activation Energy of Gate Reliability in Schottky-Gate p-GaN HEMTs: Combined Gate Leakage Current Modeling and Spectral Electroluminescence Investigation,” in *IEEE Journal of the Electron Devices Society*, vol. 12, pp. 703–709, 2024, doi: 10.1109/JEDS.2024.3454334.

[13] S. Stoffels et al., “Perimeter Driven Transport in the p-GaN Gate as a Limiting Factor for Gate Reliability,” 2019 IEEE International Reliability Physics Symposium (IRPS), Monterey, CA, USA, 2019, pp. 1–10, doi: 10.1109/IRPS.2019.8720411.

[14] M. Meneghini et al., "Degradation of GaN-HEMTs with p-GaN Gate: Dependence on temperature and on geometry," 2017 IEEE International Reliability Physics Symposium (IRPS), Monterey, CA, USA, 2017, pp. 4B-5.1–4B-5.5, doi: 10.1109/IRPS.2017.7936311.

[15] Materials To Device Simulation | Applied Materials, https://www.appliedmaterials.com/il/en/semiconductor/ginestra-software.html

[16] L. Zhang et al., “p-GaN Gate HEMT with surface reinforcement for enhanced gate reliability,” *IEEE Electron Device Lett.*, vol. 42, no. 1, pp. 22–25, Jan. 2021, doi: 10.1109/LED.2020.3037186.

[17] L. Zhang et al., “Characterization of GaON as a surface reinforcement layer of p-GaN in Schottky-type p-GaN gate HEMTs,” *Appl. Phys. Lett.*, vol. 119, no. 5, p. 053503, 2 Aug. 2021, doi: 10.1063/5.0053252.

[18] J. W. McPherson, J.-Y. Kim, A. Shanware, and H. C. Mogul, “Thermochemical description of dielectric breakdown in high dielectric constant materials,” *Appl. Phys. Lett.*, vol. 82, no. 13, pp. 2121–2123, Mar. 2003, doi: 10.1063/1.1565180.

[19] A. Padovani, D. Z. Gao, A. L. Shluger, and L. Larcher, “A microscopic mechanism of dielectric breakdown in SiO_2 films: An insight from multi-scale modeling,” *J. Appl. Phys.*, vol. 121, no. 15, p. 155101, Apr. 2017, doi: 10.1063/1.4979915.

[20] D. Cornigli, H. Schlichting, T. Becker, L. Larcher, J. T. Erlbacher, and M. Pešić, “Modelling-augmented failure diagnostics in planar SiC MOS devices using TDDB measurements,” *Solid State Phenomena*, vol. 361, pp. 93–98, Aug. 2024, doi: 10.4028/p-jbV5Vq.